

Nonlinear Residual Prediction Method for Site Based on Lasso Regression and Monte Carlo Sampling

Wang Yushi^{1,2}, Chen Zelong^{1,*}

¹College of Architecture and Civil Engineering, Beijing University of Technology, Beijing, 100124, China

²Key Laboratory of Urban Security and Disaster Engineering, Ministry of Education, Beijing, 100124, China

*Corresponding Author

Keywords: Field Effect; Equivalent Linearization; Lasso Regression; Residual Analysis

Abstract: Local ground effects exert significant modulation on seismic motion characteristics. Traditional one-dimensional equivalent linearization methods exhibit severe high-frequency "over-damping" phenomena under strong earthquake strains, while quantifying nonlinear residual responses remains challenging due to multidimensional coupling effects from seismic sources, paths, and spectral characteristics. Leveraging massive strong ground motion records from Japan's KiK-net network, this study proposes a machine learning-based approach for nonlinear system deviation prediction and uncertainty quantification through feature dimensionality reduction and probabilistic sampling. First, 15 multidimensional physical parameters encompassing seismic sources, paths, and ground motion responses were extracted. The Lasso regression algorithm (with L1 regularization) was employed for dynamic feature ± 1 optimization and dimensionality reduction to construct a multivariable nonlinear residual prediction model. Residual prediction was further implemented using Monte Carlo (MC) sampling combined with Jaccard similarity index. Results demonstrate that dominant nonlinear residual parameters exhibit distinct frequency-dependent behaviors: high-frequency components are controlled by input intensity (e.g., peak response spectra under underground conditions), while mid-to-long periods are governed by spectral evolution characteristics (e.g., average period). Compared to traditional single-parameter empirical models, the Lasso multivariable model significantly improves full-cycle prediction accuracy. MC-sampled multiple standard deviations objectively reconstruct ground response uncertainties while maintaining high Jaccard similarity with real observation datasets. This study effectively compensates for high-frequency energy misconsumption in one-dimensional theories, providing a reliable data-driven approach for accurate residual estimation.

1. Introduction

Local site effects induced by specific site conditions exert significant modulation on seismic motion characteristics. Shallow surface weak overburden layers not only substantially amplify ground motion intensity but also dramatically alter spectral composition and duration characteristics, thereby

exacerbating structural damage in engineering structures. Therefore, accurate characterization and quantification of local site effects remain indispensable core components in both seismic design and site-related probabilistic seismic hazard assessments.

Empirical methods for evaluating site effects based on strong ground motion records primarily include the Standard Spectral Ratio Method (SSR), Generalized Inversion Method (GIT), and Surface/Downhole Spectral Ratio Method (SBSR). The SSR, proposed by Borcherdt (1970) [1], compares the Fourier spectrum of soil layers with adjacent bedrock spectra to eliminate source and path effects. While this method offers clear physical interpretation and reliable results, its practical application is limited by the requirement for ideal bedrock reference sites. Andrews (1986) [2] introduced the GIT, which simultaneously separates source, path, and site effects through simultaneous multi-seismic multi-station observation equations, effectively overcoming traditional method dependencies on reference sites. The SBSR employs borehole-bottom bedrock as the reference site, where both surface and downhole records share identical source and path effects during the same earthquake, enabling more accurate characterization of site conditions' impact on seismic motion characteristics. However, this method requires consideration of destructive interference between upbound and downbound waves at bedrock interfaces. Such interference creates "spectral holes" in downhole bedrock seismic motion spectra at specific frequencies, leading to pseudo-resonance phenomena in spectral ratios. Steidl et al. (1996) [3] demonstrated that cross-spectral techniques can effectively mitigate interference effects on site response estimation.

The SBSR method utilizing vertical array systems employs the bedrock at borehole bottoms as reference points, enabling absolute control over focal and path effects within the same seismic event. This approach is widely recognized as the most direct and accurate means of characterizing local site effects. However, since purely empirical methods heavily rely on extensive strong-motion records from specific stations, both academic and engineering communities typically adopt one-dimensional equivalent linearization-based numerical simulations (e.g., SHAKE) as core assessment tools in practical engineering applications.

Although one-dimensional numerical simulations are widely used, they exhibit significant systematic physical deviations under strong earthquake-induced large strain conditions. Constrained by simplified assumptions in soil constitutive models, traditional one-dimensional theories often demonstrate "over-damping" effects at high frequencies, leading to severe underestimation of high-frequency energy. More complexly, the nonlinear residual of ground response (i.e., the deviation between measured and simulated spectral ratios) is not a static constant but rather subject to non-stationary coupling control influenced by multidimensional factors including focal mechanism, input intensity (PGA), spectral evolution, and duration. This study develops a quantitative residual prediction model that integrates multiple complex influencing factors.

To address the aforementioned challenges, this study proposes a site nonlinear residual correction prediction method based on machine learning feature dimensionality reduction and probabilistic sampling. The approach first leverages massive strong ground motion records from the KiK-net seismic network to extract multidimensional physical characteristics encompassing epicenters, seismic paths, and site conditions. Subsequently, the Lasso regression algorithm (with L1 regularization) is employed to dynamically reduce high-dimensional feature spaces, effectively eliminating redundant information while identifying key physical parameters that dominate residual variations across different frequency bands, thereby constructing an efficient multivariate prediction model. This research not only achieves precise data-driven compensation for high-frequency energy dissipation in one-dimensional theoretical models but also establishes a statistically robust framework for site residual correction.

2. Data and Benchmark Model

2.1 Station and Data Selection

This study validates the methodology using the HDKH06 station in Japan's KiK-net vertical array as a case study. Located on a Class SC-II seismic site ($V_{S30}=412$ m/s), the station features underground sensors buried approximately 115 meters deep. Eight hundred and five seismic events recorded between 2010 and 2020 were selected, with screening criteria including: underground PGA ≥ 0.2 cm/s² and signal-to-noise ratio ≥ 3 in the 0.1–20 Hz frequency band. The recorded data spanned intensity ranges from weak to moderate-strong earthquakes (including at least one event with PGA ≥ 50 cm/s²), providing sufficient coverage to assess nonlinear response characteristics.

2.2 Benchmark Numerical Model

The benchmark numerical model was developed using the HH (Hybrid Hyperbolic) hybrid hyperbolic nonlinear soil model proposed by Shi and Asimaki (2017) [4]. This model requires only shear wave velocity profiles as input to simultaneously capture soil small strain stiffness and ultimate shear strength, making it suitable for sites with only borehole data. Model parameter determination was based on classical empirical relationships. Soil density was estimated using the empirical model proposed by Mayne et al. (1999) [5]. Dynamic shear strength assessment employed the undrained shear strength (S_u) formula, following the standardized methodology of Ladd (1991) [6].

The core concept of the HH model involves modeling small strain and large strain segments separately. The γ_{ref} reference shear strain characterizing nonlinear degradation of small strain is calibrated using the empirical formula proposed by Darendeli (2001) [7].

$$\gamma_{ref} = [\phi_1 + \phi_2 (PI)(OCR)^{\phi_3}] (p'_{m0})^{\phi_4} \quad (1)$$

In response to the current lack of plasticity index (PI) data in KiK-net, an empirical threshold was forcibly assigned: $PI=10$ at time; $PI=$ at time; $PI=$ at time.

To address the current lack of plasticity index (PI) data for KiK-net, an empirical threshold was forcibly assigned based on V_S : $PI=10$ when $V_S < 200$ m/s; $PI=5$ when $200 < V_S \leq 360$ m/s; and $PI=0$ when $V_S > 360$ m/s [8]

Based on the aforementioned parameters, a modified Kondner-Zelasko (MKZ) small strain model is established:

$$\tau_{MKZ}(\gamma) = \frac{G_{max}\gamma}{1 + \beta(\gamma/\gamma_{ref})^s} \quad (2)$$

In the formula, the recommended $\beta=1$, $s=0.9190$ shape parameter is set to.

For the large strain stage, a flexible hyperbolic (FKZ) model is constructed to ensure stress convergence toward the shear strength τ_f :

$$\tau_{FKZ}(\gamma) = \frac{\gamma^d \mu}{\frac{1}{G_{max}} + \frac{\gamma^d \mu}{\tau_f}} \quad (3)$$

To achieve a smooth transition between the MKZ[9] and FKZ models across the full strain field, a S-shaped (sigmoid) weight transition function is introduced, with the transition rate parameter set to $a=100$.

$$w(\gamma) = 1 - \frac{1}{1 + 10^{-a \left(\log_{10} \left(\frac{\gamma}{\gamma_t} \right) - 4.039a^{-1.036} \right)}} \quad (4)$$

The total shear stress expression of the final hybrid hyperbolic (HH) model is expressed as the weighted sum of the two components:

$$\tau_{HH}(\gamma) = w(\gamma)\tau_{MKZ}(\gamma) + [1 - w(\gamma)]\tau_{FKZ}(\gamma) \quad (5)$$

In the formula, γ_t and a represent the transition strain and transition rate, respectively.

To ensure continuity and monotonicity of the model's physical mechanisms, this study employs constrained nonlinear optimization algorithms for parameter calibration. The objective function minimizes the stress area difference (i.e., residual sum of squares) before transition point γ_t , with morphological parameter d optimized within the 3σ confidence interval ($d \in [0.67, 1.39]$). The optimal transition strain γ_t is dynamically searched across a wide strain range of $[0.01\%, 3\%]$. The normalized shear modulus is ultimately derived as follows:

$$\frac{G}{G_{max}} = \frac{\tau_{HH}(\gamma)}{\gamma G_{max}} \quad (6)$$

The relationship between damping ratio and shear strain was determined using Darendeli's (2001) damping curve calculation formula.

Taking the HDKD06 station as an example, the basic soil layer information from the acquired original profiles (Table 1) can be obtained. By applying this correction method, we can calculate the nonlinear parameters of soil layers (dynamic stiffness curves and damping ratio curves) at the station site based solely on soil layer thickness and shear wave velocity. This provides reliable data for the one-dimensional soil layer numerical simulation mentioned earlier to analyze soil layer nonlinearity. Figure 1 shows the two corresponding curves for the HDKD06 station, as depicted in Figure 1(a) and Figure 1(b).

Table 1: Soil Profile Information

soil thickness (m)	Shear wave velocity (m/s)
10	280
8	460
18	610
48	790
26	980

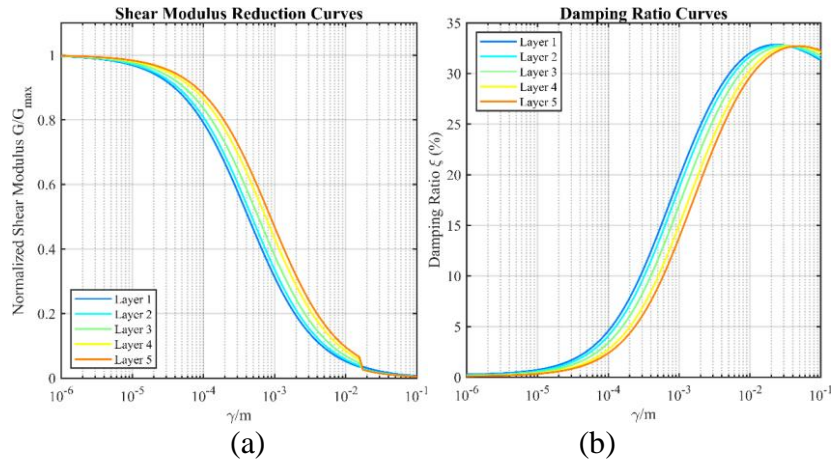


Figure 1: Dynamic stiffness curve and damping ratio curve of the HDKD06 station site

2.3 Numerical Simulation and Residual Definition

The one-dimensional equivalent linearized ground response analysis was conducted using PySeismoSoil (Shi et al., 2025) [10]. With downhole records as input and combined with borehole profiles, the surface acceleration time history was calculated to derive the simulated spectral ratio.

$$AF_{\text{sim}}(T) = \frac{S_a^{\text{sim}}(T)}{S_a^{\text{borehole}}(T)} \quad (7)$$

In the formula, $S_a^{\text{sim}}(T)$ denotes the simulated surface acceleration response spectrum, while $S_a^{\text{borehole}}(T)$ represents the measured downhole acceleration response spectrum (both with damping ratios of 5%). The measured spectrum ratio is directly calculated from on-site records:

$$AF_{\text{obs}}(T) = \frac{S_a^{\text{surface}}(T)}{S_a^{\text{borehole}}(T)} \quad (8)$$

To quantify the systematic bias of one-dimensional equivalent linearization methods $\varepsilon(T)$ in predicting site amplification effects, the spectral ratio residual is defined as the logarithmic ratio of measured spectral ratios to simulated spectral ratios:

$$\varepsilon(T) = \ln \left(\frac{AF_{\text{obs}}(T)}{AF_{\text{sim}}(T)} \right) \quad (9)$$

This residual has the following physical meaning:

$\varepsilon(T)=0$: Simulated values match measured values;

$\varepsilon(T)<0$: The simulated spectral ratio exceeds the measured one, indicating that the simulation overestimates site amplification.

$\varepsilon(T)>0$: The simulated spectral ratio is lower than the measured one, indicating that the simulation underestimates site amplification.

3. Core Methodology

3.1 Dimensionality Reduction and Feature Selection Based on Lasso Regression for Influencing Factors

To address the multidimensional complexity of seismic response analysis, this study initially identified 15 influential factors reflecting source characteristics, path effects, and site features. These factors include: intensity-related parameters such as Peak Ground Acceleration (PGA), PGA/Peak Ground Velocity (PGV) ratio, Arias intensity, and Asb (well response spectrum peak); spectral characteristics including Tsb (well response spectrum peak period), Afb (well Fourier spectrum peak), Tfb (well Fourier spectrum peak period), Tfmean (period corresponding to Fourier spectrum average frequency), bandwidth Bw, and high-frequency attenuation parameter kappa; duration-related characteristics like D5-95; as well as site resonance and refined response indicators such as Tpre (peak period ratio of onshore-to-offshore acceleration response spectra), Apre (peak ratio of onshore-to-offshore acceleration response spectra), and Rbpeak (peak frequency band energy proportion of underground responses).

Given the potential high multicollinearity among the aforementioned physical parameters, this study introduces the Lasso regression formula [11]. By incorporating an L1 regularization penalty term into the objective function, Lasso achieves automatic feature selection and dimensionality reduction for impact factors at each periodic point. This approach not only eliminates redundant features with negligible residual contribution but also precisely identifies key physical quantities that dominate nonlinear deviations across different periodic frequency bands, thereby constructing a

sparse and robust predictive model.

$$\hat{\beta}^{Lasso} = \underset{\beta}{\operatorname{argmin}} \left\{ \sum_{i=1}^n \left(y_i - \sum_{j=1}^p x_{ij} \beta_j \right)^2 + \lambda \sum_{j=1}^p |\beta_j| \right\} \quad (10)$$

In the formula:

y_i is the response variable for the i sample (e.g., spectral ratio residual).

x_{ij} denotes the j predictor variable (e.g., $\ln(PGA)$, period (T), etc.) for the i sample.

β_j is the regression coefficient of the j variable

$\lambda \geq 0$ is the penalty parameter, controlling the regularization strength.

n is the sample size, and p is the number of predictor variables.

Figures 2 and 3 demonstrate the residuals of station HDKH06 at periods $\varepsilon(T)$ of 0.1s and 3.0s. The parameter λ , determined through preliminary experiments, is set to a value between 0 and 0.15, with 300 uniformly distributed data points in logarithmic coordinates. As λ increases, the regression coefficients of all parameters exhibit corresponding variations, with similar patterns observed for other period points.

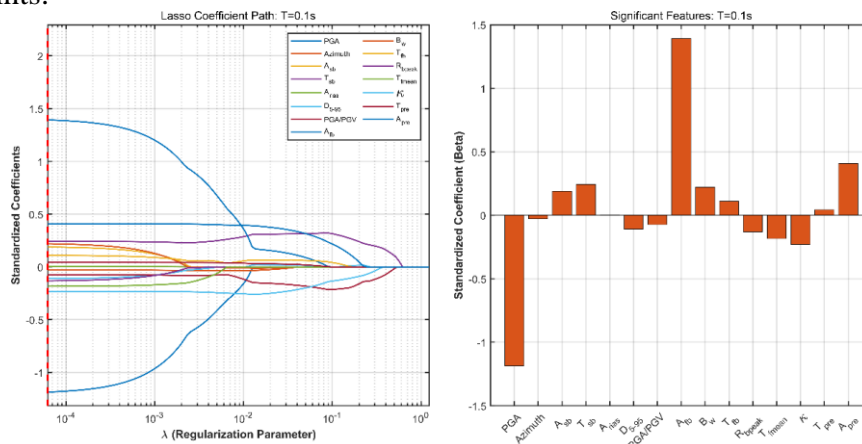


Figure 2: Variation of lasso regression coefficients at the periodic point $T=0.1s$

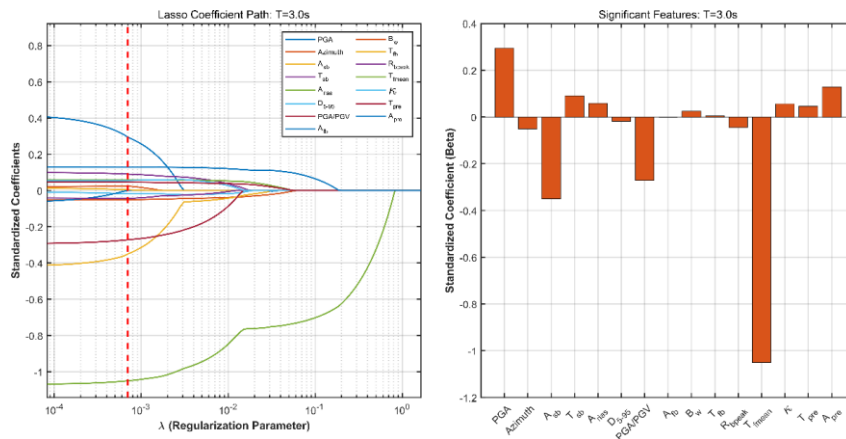


Figure 3: Variation of lasso regression coefficients at the periodic point $T=3.0s$

3.2 Prediction of Residual Nonlinear Regression Model Considering Multiple Factors

A multivariate nonlinear regression model was established based on the core influencing factors reduced by the Lasso algorithm, as shown in the following equation:

$$\varepsilon(T)=\beta_0(T)+\sum_{i=1}^n\beta_i\ln(x_i)+\sum_{i=1}^n\sum_{j+1}^n\beta_{ij}(T)\ln(IM_iIM_j)+\sum_{i=1}^n\beta_{ii}\ln(x_i^2) \quad (11)$$

In the formula, $\varepsilon(T)$ represents the ground response spectrum residual of a single seismic event at a specific period T ; $\beta_0(T)$, β_i and β_{ij} denote the regression coefficients for the constant term, first-order term, and second-order term, respectively. x_i and x_j represent the characteristic parameters of the i and j influencing factors respectively, with n taking the value of 4 (i.e., the number of key variables retained after feature selection). IM_i denotes the characteristic parameter of the i influencing factor. Taking the classical station HDKD06 as an example (Figure 4), for residual prediction at $T=0.1s$, the reduced influencing factors include A_{fb} (peak value of downhole Fourier spectrum), PGA (peak acceleration magnitude), A_{pre} (peak value of on/off well acceleration response spectrum ratio), and T_{sb} (peak value of downhole response spectrum). For residual prediction at $T=0.3s$, the reduced factors are A_{fb} (peak value of downhole Fourier spectrum), PGA (peak acceleration magnitude), A_{pre} (peak value of on/off well acceleration response spectrum ratio), and T_{sb} (period of downhole response spectrum peak). At $T=0.1s$, the reduced parameters include A_{fb} (peak value of downhole Fourier spectrum), PGA (peak acceleration magnitude), A_{pre} (peak value of on/off well acceleration response spectrum ratio), and PGA/PGV (ratio of peak acceleration to peak velocity). For $T=0.3s$, the reduced factors consist of T_{fmean} (period corresponding to average Fourier spectrum frequency), PGA (peak acceleration magnitude), A_{sb} (peak value of downhole response spectrum), and PGA/PGV (ratio of peak acceleration to peak velocity). σ represents standard deviation. Table 2 presents the multivariate nonlinear regression coefficients obtained from the residual curve of station HDKH06 at periods of 0.1s, 0.3s, 1.0s, and 3.0s.

Table 2: (HDKH06) Values of each regression coefficient in the multivariate nonlinear regression model for each period point of the residual curve

coefficient	0.1015	0.3027	0.9917	2.9584
β_0	-1.1799	0.3883	-1.3880	-0.8566
β_1	0.5094	1.0145	0.6585	0.8826
β_2	-0.3245	-0.9611	-0.4196	-0.7087
β_3	0.6758	-0.6734	1.1044	0.4768
β_4	0.7030	1.4510	0.1626	0.2120
β_{12}	0.3391	0.5438	0.0572	0.2888
β_{13}	0.2016	0.1172	-0.2837	-0.1836
β_{14}	-0.4250	-0.7066	-0.0385	-0.3029
β_{23}	-0.2083	-0.0885	0.2239	0.1413
β_{24}	0.3455	0.6247	0.0185	0.2626
β_{34}	0.1238	-0.0190	-0.1151	0.0804
β_{11}	-0.2050	-0.2993	-0.0437	-0.1510
β_{22}	-0.1363	-0.2509	-0.0086	-0.1390
β_{33}	-0.0706	0.1831	-0.1136	-0.0900
β_{44}	-0.3216	-0.4308	0.0298	-0.0897
σ	0.2412	0.2021	0.1596	0.1796

Figure 4 below illustrates the correlation between the predicted residual values at various periodic points calculated based on the aforementioned parameters and their corresponding residuals from the multivariate nonlinear fitting.

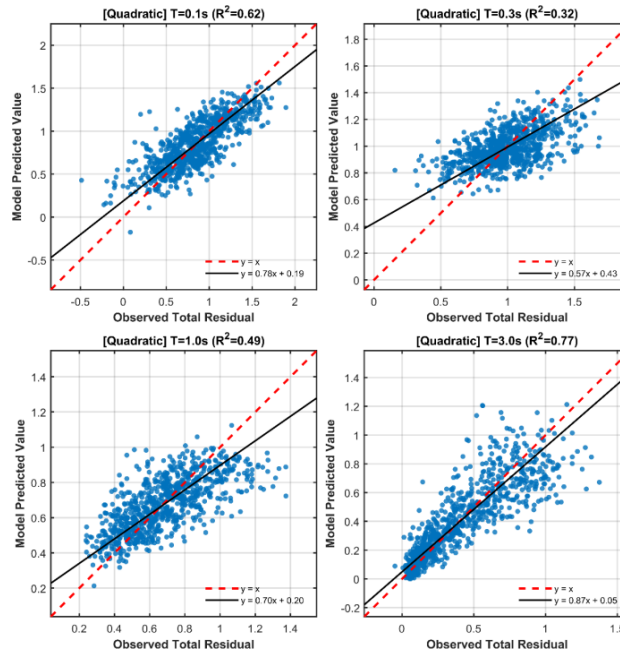


Figure 4: Comparison of linear regression predicted values versus fitted values for residual at four cycle points

3.3 Nonlinear Prediction of Residuals Based on Monte Carlo (MC) Sampling

The deterministic component of the $\alpha_0 + \sum \alpha_i \ln x_i$ regression equation extracts the conditional mean trend of ground motion residuals, reflecting common patterns across multiple samples. However, real ground motion spectra are not perfectly smooth but exhibit high-frequency oscillations caused by complex wave propagation paths. Direct application of excessively smoothed mean prediction curves to artificial seismic wave synthesis would lead to severe underestimation of high-frequency dynamic responses in engineering structures. To address this, our study builds upon deterministic prediction by employing Monte Carlo sampling [12] to reconstruct the stochastic uncertainty of residual sequences.

Specifically, Gaussian random sequences conforming $\sigma(T)$ to a given variance distribution are generated based on the standard deviations extracted from regression models at various frequency points. After frequency-band-specific smoothing processing, these sequences are superimposed onto the baseline prediction curve. This approach is not designed to fit a specific historical earthquake event, but rather aims to generate data with authentic physical variance characteristics.

When evaluating model prediction performance (as demonstrated in the coefficient of determination comparison shown in Figure 5 below), it becomes evident that Monte Carlo sampling [9] reconstructed curves exhibit universally lower point-to-point R^2 values compared to linear and nonlinear regression models, with some frequency bands even displaying negative values. This phenomenon does not indicate model accuracy degradation but rather represents the inherent mathematical cost of reconstructing physical variance. From a mathematical fitting perspective, regression analysis optimizes the sum of squared residuals (SSR), whose mean curves inherently intersect the data centroid, thus achieving the highest R^2 values. However, Monte Carlo sampling fundamentally involves "variance injection," introducing stochastic fluctuations (spikes) representing uncertainty onto smoothed mean lines. When performing point-by-point residual calculations between simulated curves containing random phase components and individual observed curves, absolute alignment of local extremum points at specific frequency points becomes impossible,

inevitably leading to increased mathematical SSR values and reduced R^2 as depicted in Figure 5.

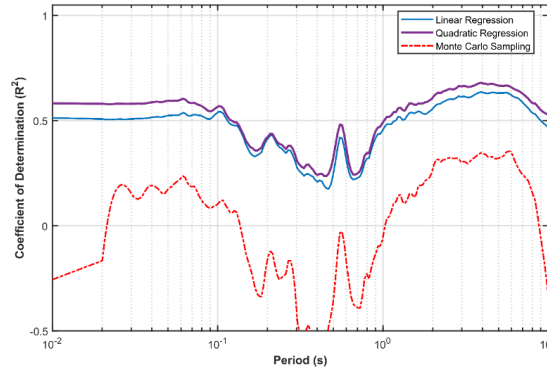


Figure 5: Comparison of coefficient of determination for three methods

Figure 6 compares residual curves derived from double spectral ratios of random strong vibration records at several HDKH06 stations with their predicted curves. The black line represents acceleration response spectra calculated from vibration records, the blue line shows linear regression predictions, the purple segment indicates quadratic regression predictions, and the red line presents Monte Carlo-sampled predictions based on quadratic regression curves.

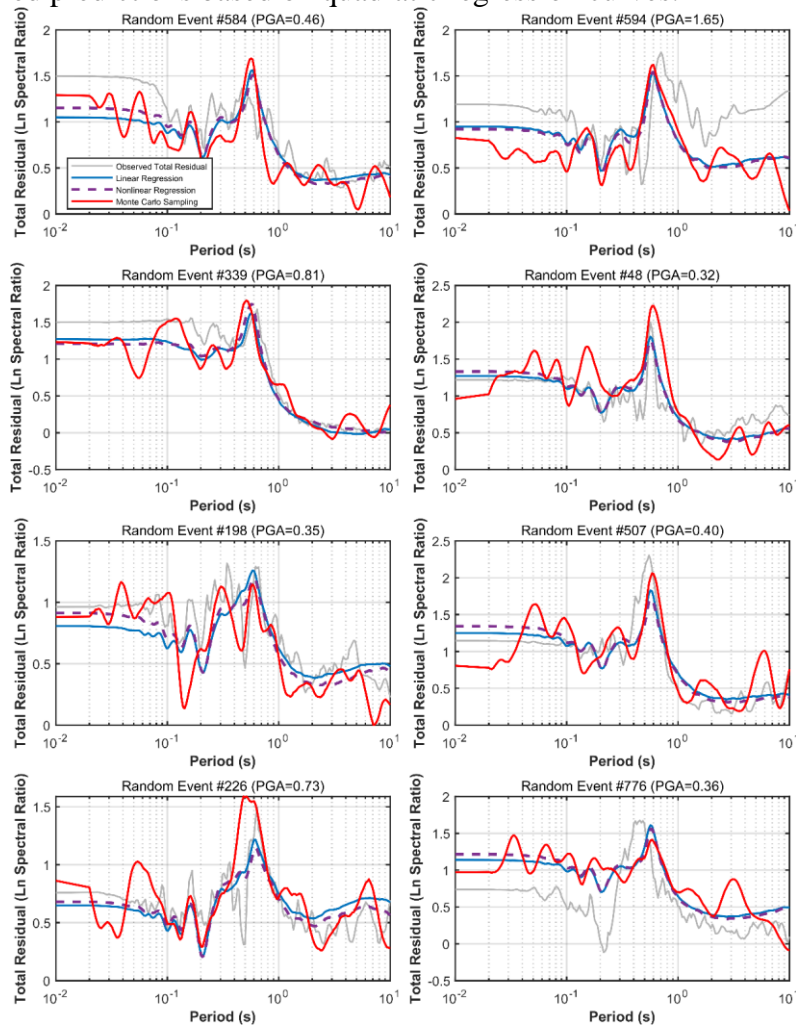


Figure 6: Comparison of residual curves obtained from several double spectral ratios with their predicted curves

4. Results and Discussion

4.1 Lasso Dimensionality Reduction Results and Key Feature Analysis

To address multicollinearity among 15 candidate input factors, this study utilized the L1 regularization property of Lasso regression to perform dynamic dimensionality reduction and sparsification on feature vectors across different periodic points. Analysis results (shown in Figures 2 and 3) reveal distinct frequency-dependent characteristics of dominant physical quantities governing nonlinear ground motion residuals: At high frequencies ($T=0.1s$), indicators representing absolute seismic intensity and energy (e.g., Afb, PGA) exhibit dominant weighting patterns. This aligns with classical soil dynamics principles: intense input energy directly induces strong nonlinear behavior in shallow soil layers (shear modulus attenuation and abrupt damping ratio spikes), while one-dimensional equivalent linearization models frequently produce "over-damping" phenomena at this frequency range, leading to severe underestimation of high-frequency energy and significant prediction residuals. In medium-to-long period frequency bands ($T=3.0s$), spectral evolution parameters (e.g., T_{fmean} , PGA/PGV) demonstrate markedly increased weighting coefficients. These findings indicate that for deep overburden layers or sites prone to low-frequency resonance, the frequency composition of seismic waves and their duration critically govern cumulative energy dissipation and residual distribution in deep soil media.

4.2 Precision Validation of Nonlinear Residual Prediction Model

After identifying optimal feature subsets for each cycle, this study compared prediction residuals with actual observed residuals using multivariate regression models. Figure 4 demonstrates residual fitting performance of target stations (e.g., HDKH06) on validation sets. Results show: The 0.1-second trendline function $y=0.7+0.19$ achieves a coefficient of determination (R^2) of 0.62 between predicted and fitted residuals; the 0.3-second trendline function $y=0.5+0.43$ yields $R^2=0.32$; the 1.0-second trendline function $y=0.2$ demonstrates $R^2=0.49$; while the 3-second trendline function $y=0.8+0.05$ achieves $R^2=0.77$, indicating improved prediction accuracy compared to linear regression results. Compared to traditional single-parameter PGA empirical correction models, the Lasso feature selection-based multivariate prediction model exhibits superior generalization capabilities. Prediction residuals closely align with real observation values in mid-to-high frequency bands, with R^2 values consistently maintained at high levels. These findings conclusively demonstrate that data-driven models incorporating multidimensional source and path influence factors can effectively correct systematic biases in one-dimensional theoretical models during strong earthquake strain phases, while compensating for seismic energy losses caused by theoretical model inaccuracies. Figure 6 presents the comparison between residual curves derived from the double spectral ratios of random strong vibration records from several HDKH06 stations and their predicted curves. This visualization demonstrates the method's applicability and provides valuable reference for subsequent research.

4.3 Post-Monte Carlo Sampling Accuracy Verification

Figure 5 demonstrates that Monte Carlo sampling effectively reproduces the inherent "physical wave characteristics" of single seismic motions compared to traditional ordinary least squares methods. By calculating the Jaccard similarity coefficient [13] between the predicted residual curves and actual residuals at station HDKH06 (Figure 7), the median value of the predicted residual boxplot approaches 0.90. This statistically confirms that the current prediction model exhibits excellent baseline fitting accuracy at this station, with the overall waveform and amplitude overlap of residual spectra reaching high confidence levels, indicating relatively reliable prediction performance.

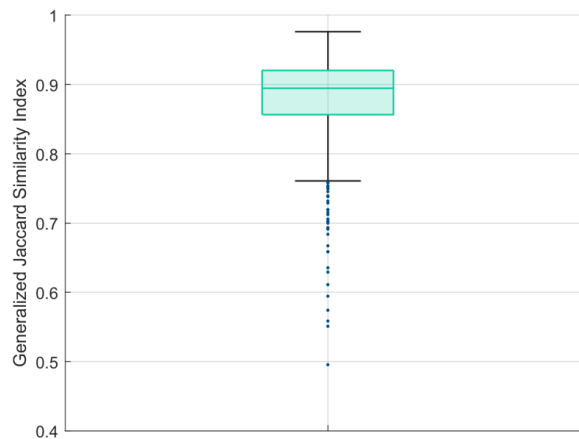


Figure 7: Box plot of Jaccard similarity coefficient for HDKH06 station

References

- [1] Borcherdt R D. *Effects of local geology on ground motion near San Francisco Bay*[J]. *Bulletin of the Seismological Society of America*, 1970, 60(1): 29-61.
- [2] Andrews, D.J. (1986). *Objective determination of source parameters and similarity of earthquakes of different size*. *Earthquake Source Mechanics*.
- [3] Steidl, J.H., Tumarkin, A.G., & Archuleta, R.J. (1996). *What is a reference site?* *Bulletin of the Seismological Society of America*, 86(6), 1733-1748.
- [4] Shi Y, Asimaki D. *A hysteretic–hyperbolic model for site response analysis*[J]. *Earthquake Engineering & Structural Dynamics*, 2017, 46(13): 2137-2155.
- [5] Mayne P W, Schneider J A, Martin G K. *Small-and large-strain soil properties from seismic flat dilatometer tests*[C]//*Proc. 2nd Int. Symp. on Pre-Failure Deformation Characteristics of Geomaterials*. 1999: 419-427.
- [6] Ladd C C. *Stability evaluation during staged construction*[J]. *Journal of geotechnical engineering*, 1991, 117(4): 540-615.
- [7] Darendeli M B. *Development of a new family of normalized modulus reduction and material damping curves*[M]. *The university of Texas at Austin*, 2001.
- [8] Zalachoris, Georgios. *Evaluation of one-dimensional siteresponse methodologies using borehole arrays*. *Diss.* 2014.
- [9] Matasović N, Vucetic M. *Cyclic characterization of liquefiable sands*[J]. *Journal of Geotechnical Engineering*, 1993, 119(11): 1805-1822.
- [10] Shi, J., Asimaki, D., Li, W., & Xia, F. (2025). *PySeismoSoil: A Python library for 1D seismic site response analysis (Version v0.6.3)* [Computer software]. Zenodo.
- [11] Tibshirani R. *Regression shrinkage and selection via the lasso*[J]. *Journal of the Royal Statistical Society Series B: Statistical Methodology*, 1996, 58(1): 267-288.
- [12] Liu J S, Liu J S. *Monte Carlo strategies in scientific computing*[M]. *New York: springer*, 2001.
- [13] Jaccard P. *Distribution de la flore alpine dans le bassin des Dranses et dans quelques régions voisines*[J]. *Bull Soc Vaudoise Sci Nat*, 1901, 37: 241-272.